

NEW NEAR-INFRARED SPECTROSCOPY OF THE HIGH-REDSHIFT QUASAR B1422+231 AT $z = 3.62$

TAKASHI MURAYAMA¹ AND YOSHIAKI TANIGUCHI¹

Astronomical Institute, Tohoku University, Aoba, Sendai 980-8578, Japan; murayama@astr.tohoku.ac.jp, tani@astr.tohoku.ac.jp

AARON S. EVANS¹

Department of Astronomy, California Institute of Technology, Mail Stop 105-24, Pasadena, CA 91125; ase@astro.caltech.edu

D. B. SANDERS AND K.-W. HODAPP

Institute for Astronomy, University of Hawaii, 2680 Woodlawn Drive, Honolulu, HI 96822; sanders@ifa.hawaii.edu, hodapp@ifa.hawaii.edu

AND

KIMIYAKI KAWARA AND NOBUO ARIMOTO

Institute of Astronomy, University of Tokyo, 2-21-1 Osawa, Mitaka, Tokyo 181-8588, Japan;

kkawara@mtk.ioa.s.u-tokyo.ac.jp, arimoto@mtk.ioa.s.u-tokyo.ac.jp

Received 1998 April 27; accepted 1998 December 16

ABSTRACT

We present new near-infrared (rest-frame UV-to-optical) spectra of the high-redshift, gravitationally lensed quasar B1422+231 ($z = 3.62$). Diagnostic emission lines of Fe II, O III $\lambda 5007$, and H β , commonly used to determine the excitation, ionization, and chemical abundances of radio-quiet and radio-loud quasars, were detected. Our new data show that the ratio Fe II (UV)/H $\beta = 18.1 \pm 4.6$ and Fe II (optical)/H $\beta = 2.3 \pm 0.6$ are higher than those reported by Kawara et al. by factors of 1.6 and 3.3, respectively, although the ratio [O III] $\lambda 5007$ /H $\beta = 0.19 \pm 0.02$ is nearly the same between the two measurements. The discrepancy of the line flux ratios between the measurements is likely due to improved data and fitting procedures rather than to intrinsic variability. While approximately half of the high- z quasars observed to date have much more extreme Fe II (optical)/H β ratios, the line ratio measured for B1422+231 are consistent with the observed range of Fe II (optical) ratios of low- z quasars.

Key words: quasars: emission lines — quasars: individual (B1422+231)

1. INTRODUCTION

Since near-infrared (NIR) spectroscopy of high-redshift ($z > 2$) quasars provides information about their rest-frame optical spectroscopic properties, it is now possible to systematically compare the spectroscopic properties (e.g., excitation, ionization, and chemical abundances) of high- z and low- z quasars. Although the first NIR spectroscopic observations of high- z quasars were made nearly two decades ago (Hyland, Becklin, & Neugebauer 1978; Puetter et al. 1981; Soifer et al. 1981), high-quality NIR spectra have been obtained for only ~ 10 high- z quasars to date (e.g., Carswell et al. 1991; Hill, Thompson, & Elston 1993; Elston, Thompson, & Hill 1994, hereafter ETH; Kawara et al. 1996, hereafter K96; Taniguchi et al. 1997b; Murayama et al. 1998; see also Taniguchi et al. 1997a). However, despite the relatively small number of objects observed, several very interesting properties of high- z quasars have emerged. In particular, Hill et al. (1993) and ETH suggested that unusually strong optical Fe II emission may be common in the high- z universe ($2 < z < 3.4$); to date, five out of eight high- z quasars observed have very strong optical Fe II emission with $EW(\text{Fe II})/EW(\text{H}\beta) \gtrsim 1$ (see Murayama et al. 1998). By comparison, a much smaller fraction of far-infrared (FIR) selected active galactic nuclei ($L_{\text{FIR}} \gtrsim 10^{11} L_{\odot}$) have strong optical Fe II emission (cf. Lípári, Terlevich, & Macchetto 1993).

Recently, we obtained NIR spectra of the radio-loud, flat-spectrum, high- z quasar B1422+231 (Patnaik et al. 1992; Lawrence et al. 1992) using the Mayall 4 m telescope at Kitt Peak National Observatory (KPNO) (K96). Although this quasar is at $z = 3.62$, its optical magnitude is sufficiently

bright ($m_r = 15.5$; Yee & Bechtold 1996), due to gravitational lensing (Patnaik et al. 1992; Lawrence et al. 1992), to allow it to be studied by NIR spectroscopy. The NIR spectra show that the flux ratio $F(\text{Fe II } \lambda\lambda 4434\text{--}4684)/F(\text{H}\beta)$ is much less than that of the other high- z quasars (K96) and, in fact, is similar to those of radio-loud, flat-spectrum, low- z quasars with “normal” optical Fe II emission. This suggested that high- z quasars may exhibit a range of values of $F(\text{Fe II } \lambda\lambda 4434\text{--}4684)/F(\text{H}\beta)$ similar to what has been observed for low- z quasars. In order to confirm this result, we have obtained new NIR spectra using the University of Hawaii (UH) 2.2 m telescope. In this paper, we present our new NIR spectroscopy of B1422+231 and compare it with our previous measurements.

2. OBSERVATIONS AND DATA REDUCTION

We observed B1422+231 on 1996 April 7 (UT) using the K-band spectrograph (KSPEC; Hodapp et al. 1996) at the Cassegrain focus (f/31) of the UH 2.2 m telescope in combination with the UH tip-tilt system (Jim et al. 1999). The cross-dispersed echelle design of KSPEC provided simultaneous coverage of the entire 1–2.5 μm wavelength region. The projected pixel size of the HAWAII 1024 \times 1024 array was 0".167 along the slit and $\simeq 5.6 \text{ \AA}$ at 2 μm along the dispersion direction. We used a 0".96 wide slit oriented east-west and centered on the intensity peak of component B (Patnaik et al. 1992) of B1422+231 (see Fig. 1). However, comparing the two images given in Figure 1, we find that actual light from component B is 59% of the total measured flux and the remaining 41% is associated with light contamination from components A and C. Therefore, the flux of our spectra is 1.7 times as bright as real component B flux.

Thirty exposures, each of 180 s integration, taken under

¹ Visiting Astronomer of the University of Hawaii 2.2 m telescope.

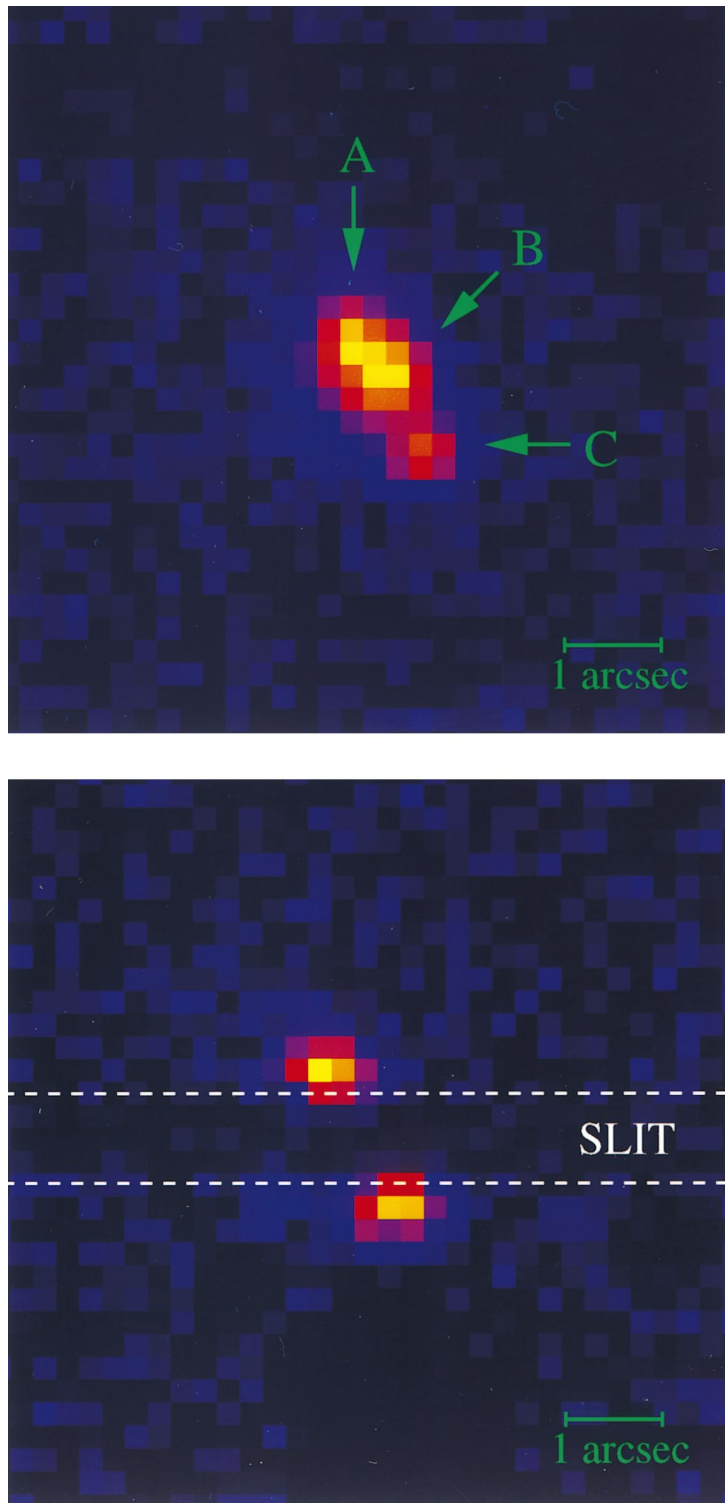


FIG. 1.—NIR (K-band) image of B1422+231 taken with the field viewer of KSPEC. The weakest component, D ($0^{\circ}94$ east and $0^{\circ}81$ south from component B), can barely be seen. In the bottom panel, we show our $1''$ slit position.

photometric conditions, were obtained by shifting the position of the object along the slit at intervals of $5''$ between each integration. The total integration time was 5400 s. An A-type standard star, HD 106965 (Elias et al. 1982), was observed for flux calibration. Another A-type star, HD 136754 (Elias et al. 1982), was also observed before and after observing B1422+231 to correct for atmospheric absorp-

tion. Spectra of an incandescent lamp and an argon lamp were taken for flat-fielding and wavelength calibration, respectively. Typical widths of the spatial profiles of the standard-star spectra were $\sim 0.5''$ (FWHM) throughout the night. Note that our previous NIR spectroscopy of this quasar at KPNO was obtained using a $1.44''$ slit under $1.4\text{--}2.1''$ seeing conditions (K96).

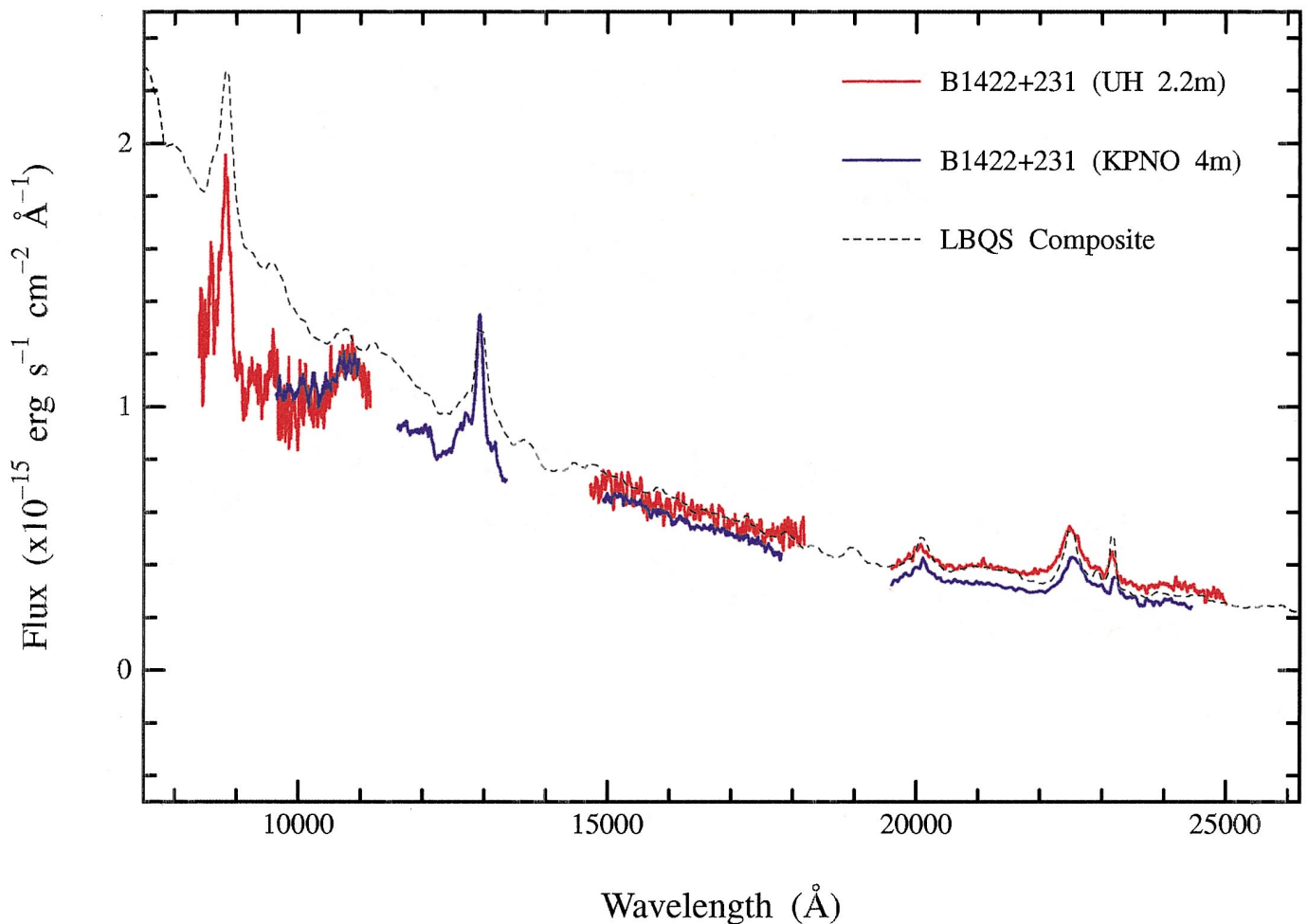


FIG. 2.—Comparison of the observed-frame *IHK* spectra of B1422+231 (red line) and both our previous measurement at KPNO (K96; blue line) and the LBQS composite spectrum of Francis et al. (1991; black-dashed line).

Data reduction was performed with IRAF² using standard procedures as outlined in Hora & Hodapp (1996). Sky and dark counts were removed by subtracting the average of the preceding and following exposures, and then the resulting frame was divided by a normalized dome flat. The target quasar was not bright enough to trace its position in each frame with sufficient accuracy. Therefore, we first fitted the spectral positions of the standard-star spectra with a third-order polynomial function that properly traces the echelle spectrum. These fitting results were then applied to the quasar spectra. Using this procedure, we extracted the quasar spectra with an aperture of 3", which was determined to be the typical width where the flux was $\sim 10\%$ of the peak flux along the spatial profile of the standard star. In order to subtract the sky emission, we used the data just adjacent to the 3" aperture. The wavelength scale of each extracted spectrum was calibrated to an accuracy of 18 km s^{-1} at $1.1 \mu\text{m}$, 20 km s^{-1} at $1.6 \mu\text{m}$, and 19 km s^{-1} at $2.0 \mu\text{m}$, based on both the argon emission lines of the calibration lamp and on the telluric OH emission lines. The spectral resolutions (FWHM) measured from the argon

lamp spectra were $\approx 500 \text{ km s}^{-1}$ at $1.1 \mu\text{m}$, $\approx 450 \text{ km s}^{-1}$ at $1.6 \mu\text{m}$, and $\approx 500 \text{ km s}^{-1}$ at $2.0 \mu\text{m}$. Finally, the spectra were median-combined in each band. Atmospheric absorption features were removed using the spectra of the A-type star HD 136754 because A-type stars are best suited for correcting for atmospheric absorption features. However, since A-type stars inherently have hydrogen recombination absorption lines (e.g., the Brackett series in *H* and *K* bands and the Paschen series in *I* and *J* bands), we removed these features using Voigt profile fitting before the correction. In order to check whether this procedure worked, we also applied the same atmospheric correction for the spectra of M-type stars whose data were obtained on the same night. Comparing our corrected spectra of the M-type stars with their published spectra (Lançon & Rocca-Volmerange 1992), we found that our correction procedure works appropriately. Finally, in order to calibrate the flux scale, we used the spectrum of the standard star HD 106965 (A2, $K = 7.315$) divided by a 9000 K blackbody spectrum, which fits the *JHK*L magnitude of the standard (Elias et al. 1982) with only 1.2% deviation. Photometric errors were determined to be less than 10% over all observed wavelengths.

3. RESULTS AND DISCUSSION

Figure 2 shows the spectra of B1422+231 (red line) in the *IHK* bands together with both our previous measurement at KPNO (blue line; K96) and the Large Bright Quasar

² Image Reduction and Analysis Facility (IRAF) is distributed by the National Optical Astronomy Observatories, which are operated by the Association of Universities for Research in Astronomy, Inc., under cooperative agreement with the National Science Foundation.

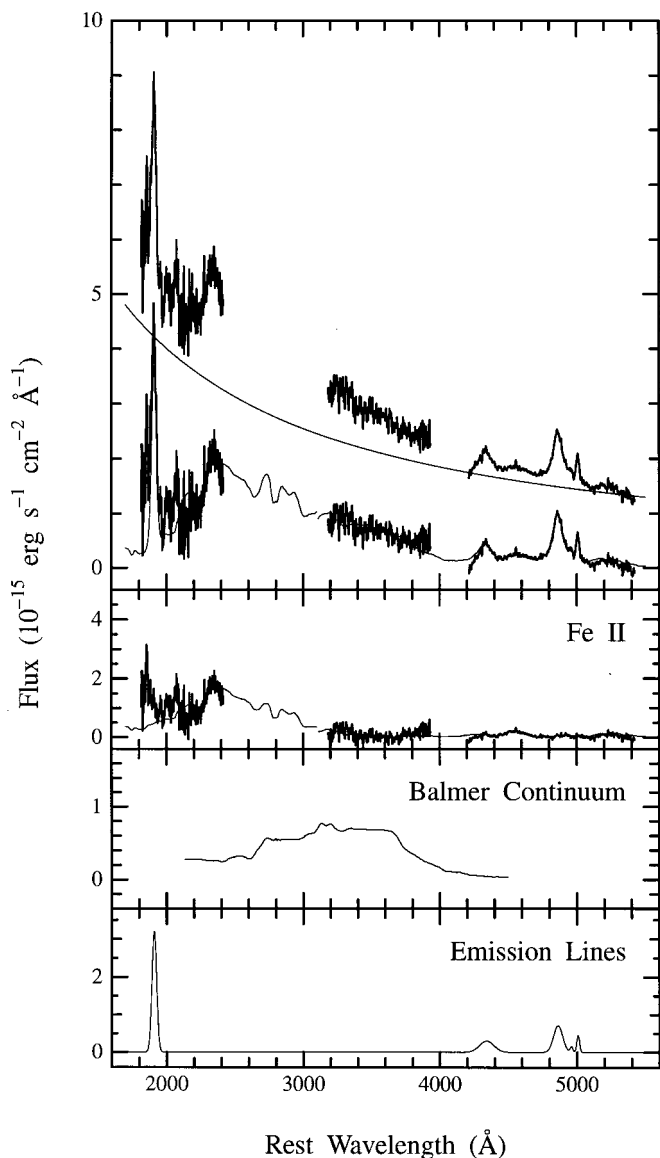


FIG. 3.—The top panel gives the rest-frame spectrum of B1422+231 and the same spectrum with the power-law continuum subtracted, together with the power-law continuum and a synthetic spectrum composed of Fe II and Balmer continuum emission plus other emission lines. Note that the rest-frame spectrum was derived by dividing the observed frame spectrum by $1+z$ after converting observed wavelengths into the rest-frame wavelengths. The spectrum shown in the panel second from the top is the extracted Fe II emission of B1422+231 together with the best-fit Fe II template. The second from bottom and bottom panels show the best-fit templates of the Balmer continuum and other emission lines, respectively.

Survey (LBQS) composite spectrum shifted to $z = 3.62$ (black-dashed line; Francis et al. 1991). Since the efficiency of KSPEC in the J -band is not high, we have not used the J -band data in this paper.

Although our new measurement was made with a narrower slit (0.96 wide) than that used by K96 (1.44 wide), the H - and K -band fluxes are slightly higher than those of the previous measurement. K96 tried to carefully correct for the effect of seeing on the relative flux calibration among the spectral bands because they could take only one band spectrum at a time. However, the time variation of the seeing in their observations made it difficult to perform the correction very accurately. Since our new I - to K -band NIR spectra were obtained simultaneously, our new measure-

ment should be more reliable than that of K96. Our new I -band spectrum detects [C III] $\lambda 1909$ emission clearly. Further, some unidentified emission features at 2000 and 2080 Å as well as the dip at 2200 Å in the rest frame, which are shown in the average spectrum of LBQS quasars (Francis et al. 1991), are also seen. The presence of [O III] $\lambda 5007$ emission has also been confirmed.

The continuum flux of component B between 1330 and 1380 Å, which was obtained by Impey et al. (1996) 13 months prior to our observations, was assumed for the continuum level on the short wavelength side of our spectra. We applied the factor 1.7 to this continuum level in order to correct the contaminated light from component A and C for our spectra (see previous section). The continuum level on the long wavelength side of our spectra was chosen by fitting a power-law continuum plus a Fe II template simultaneously to minimize the residual between 4450 and 4750 Å and beyond 5100 Å. We used the Balmer continuum template that was generated to approximate the emission-line strengths seen in 0742+318 (see Wills, Netzer, & Wills 1985, Fig. 3d). The Fe II emission profile of the very strong Fe II-emitting low-ionization broad absorption line quasar PG 0043+039 (Turnshek et al. 1994) was used as the Fe II template. Due to a relatively poor fit over the entire wavelength range when using a single template, two Fe II templates were used: one for shortward of 3000 Å and the other for longward of 3000 Å. The power-law continuum that we derive is given by $f_{\nu} \propto \nu^{-0.88}$. This spectral index is steeper than the $f_{\nu} \propto \nu^{-0.54}$ power law derived in K96. Yee & Bechtold (1996) report that B1422+231 had become brighter by 0.12 mag during 13 months (see also Kundić et al. 1997), but variability of 0.12 mag would change the spectral index to -0.88 ± 0.08 at most. Therefore, it is unlikely that the difference of the spectral index between K96 and our current work is due to the variability inherent in this quasar. Thus, we conclude that the change in the calculated spectral index is due to our improved absolute NIR spectrophotometry by simultaneous observations of IHK bands using KSPEC.

Figure 3 shows the rest-frame spectrum of B1422+231 with the power law subtracted and the best-fit synthetic spectrum composed of Fe II and Balmer continuum emission as well as other broad lines. The fluxes, equivalent widths, and line widths of the detected emission lines are summarized in Table 1 together with the previous measurements of K96. Our new data show that the ratio Fe II (UV)/ $H\beta$ and Fe II (optical: 3500–6000 Å)/ $H\beta$ are higher than those of K96 by factors of 1.6 and 3.3, respectively. These differences are mainly due to adopting the different power-law continuum described above. However, our new Fe II (optical)/ $H\beta$ ratio for B1422+231 is still in the observed range for low- z , radio-loud quasars (Boroson & Green 1992; see Taniguchi et al. 1997b; Murayama et al. 1998). The [O III] $\lambda 5007/H\beta$ ratio is nearly the same between the two measurements. We also note that there appears to be evidence for excess emission at $\lambda < 2100$ Å in the rest frame (see Fig. 3, *second from top*).

Our new measurements yield a flux ratio of Fe II (UV)/Fe II (optical) $\simeq 8.0$. Since Wills et al. (1985) give a range of $4 < \text{Fe II (UV)/Fe II (optical)} < 12$ for low- z quasars, B1422+231 is typical of low- z quasars in this respect. We also obtain a flux ratio of Fe II (optical: 4484–4684 Å)/ $H\beta \simeq 0.53$, which is significantly smaller than the range of values (~ 1.5 – 2) found by Hill et al. (1993) for quasars with

TABLE 1
COMPARISON OF EMISSION-LINE PROPERTIES OF B1422+231

LINE	$F/F(H\beta)$		EW(rest) ^a (Å)		FWHM _{cor} ^b (km s ⁻¹)	
	K96	This Study	K96	This Study	K96	This Study
Global power-law continuum:						
[C III] λ 1909	2.31 ± 0.50	...	32.2 ± 6.8	...	6260
Mg II λ 2798	0.97 ± 0.06	...	19.5	...	2500	...
[O III] λ 3727	<0.04 ^c	<0.09 ^c	<1.1 ^c	<2.6 ^c	(1000)	(1000)
H γ + [O III] λ 4363	0.28 ± 0.04	0.68 ± 0.17	10.6	23.4 ± 5.8	3500	8635
H β	1	1 ^d	44.9	39.6 ± 2.3	4786	4786
[O III] λ 5007	0.20 ± 0.02	0.19 ± 0.02	9.2	8.0 ± 0.7	840	1357
Fe II UV ^e	11.2 ± 3.5	18.1 ± 4.6	...	340 ± 85
Fe II optical ^f	0.68 ± 0.22	2.26 ± 0.62	...	86 ± 23
Fe II optical ^g	0.53 ± 0.15	...	20 ± 5
Balmer continuum	6.91 ± 1.17	9.4 ± 1.9
Local linear continuum: ^h						
H γ + [O III] λ 4363	0.20 ± 0.05	...	8.2 ± 2.1	...	4108
H β	1 ⁱ	...	48.5 ± 3.0	...	5591
[O III] λ 5007	0.20 ± 0.02	...	10.3 ± 1.0	...	1671
Fe II optical ^f	0.57 ± 0.46	...	26.8 ± 21.9
Fe II optical ^g	0.13 ± 0.11	...	5.9 ± 4.8

^a Rest-frame equivalent width.

^b FWHM corrected for instrumental broadening.

^c 3σ upper limits, assuming FWHM_{cor} = 1000 km s⁻¹.

^d $F(H\beta) = (5.9 \pm 0.3) \times 10^{-14}$ ergs s⁻¹ cm⁻².

^e Fe II UV $\lambda\lambda$ 2000–3000, for comparison with the results of Wills et al. 1985.

^f Fe II optical $\lambda\lambda$ 3500–6000 for comparison with the results of Wills et al. 1985.

^g Fe II optical $\lambda\lambda$ 4434–4684 for comparison with the results of Hill et al. 1993.

^h See Appendix.

ⁱ $F(H\beta) = (7.8 \pm 0.5) \times 10^{-14}$ ergs s⁻¹ cm⁻².

$z \simeq 2$ –2.5. This demonstrates that it is perhaps dangerous to attempt a measurement of the iron abundance using solely optical Fe II emission features, as suggested by Wills et al. (1985).

Finally, we speculate about the formation epoch of the host galaxy of B1422+231. Our new measurement has confirmed that the Fe II (total)/H β ratio for B1422+231 is higher than normal with respect to what is found for low- z quasars. Since the low- z quasars are believed to be associated with nuclei of massive galaxies, their chemical abundances are expected to be higher than or roughly equal to solar. Therefore, the observed higher Fe II (total)/H β ratio suggests that the iron abundance of B1422+231 is at least comparable to the solar value. If this is the case, it is expected that the majority of iron would come from Type Ia supernovae. Yoshii, Tsujimoto, & Nomoto (1996) derived ~ 1.5 Gyr for the lifetime of SN Ia progenitors from an analysis of the O/Fe and Fe/H abundances in solar neigh-

borhood stars. If the Fe enrichment started at 1.5 Gyr after the onset of the first epoch of star formation, the host galaxy of B1422+231 would have formed at $z \sim 9$ or earlier for $q_0 = 0.0$ and $H_0 = 75$ km s⁻¹ Mpc⁻¹ (K96).

We are very grateful to the staff of the UH 2.2 m telescope. In particular, we would like to thank Andrew Pickles for his technical support and assistance with the observations. This work was financially supported in part by Grants-in-Aid for Scientific Research (Nos. 07044054 and 09640311) from the Japanese Ministry of Education, Science, Sports, and Culture and by the Foundation for Promotion of Astronomy, Japan. T. M. is thankful for support from a Research Fellowship from the Japan Society for the Promotion of Science for Young Scientists. This research has made use of the NASA/IPAC Extragalactic Database (NED) and the NASA Astrophysics Data System Abstract Service.

APPENDIX

COMMENTS ON CONTINUUM FITTING

In our spectral fitting procedure, we have used the global continuum that was determined using the continuum from the rest-frame UV to optical. However, local continua have often been used to measure the optical Fe II/H β ratio for low- z quasars because of the lack of rest-frame UV spectra (e.g., Boroson & Green 1992). Since the adopted continuum affects the measurements of emission-line fluxes (see Murayama et al. 1998), we examine such differences in the flux measurement for the case of B1422+231. In Figure 4, we show the spectral fitting results for both global continuum and the local continuum cases. It is shown that the local continuum fit tends to give lower fluxes for the concerned emission lines; the measured fluxes for H γ + [O III] λ 4363, H β , [O III] λ 5007, and optical Fe II are given in Table 1. Comparing these fluxes with those measured using a global fit to the continuum, we find that the optical Fe II flux based on the local continuum is 4 times lower than that determined using a global continuum fit, although the [O III] λ 5007 flux is nearly the same using both the local and global

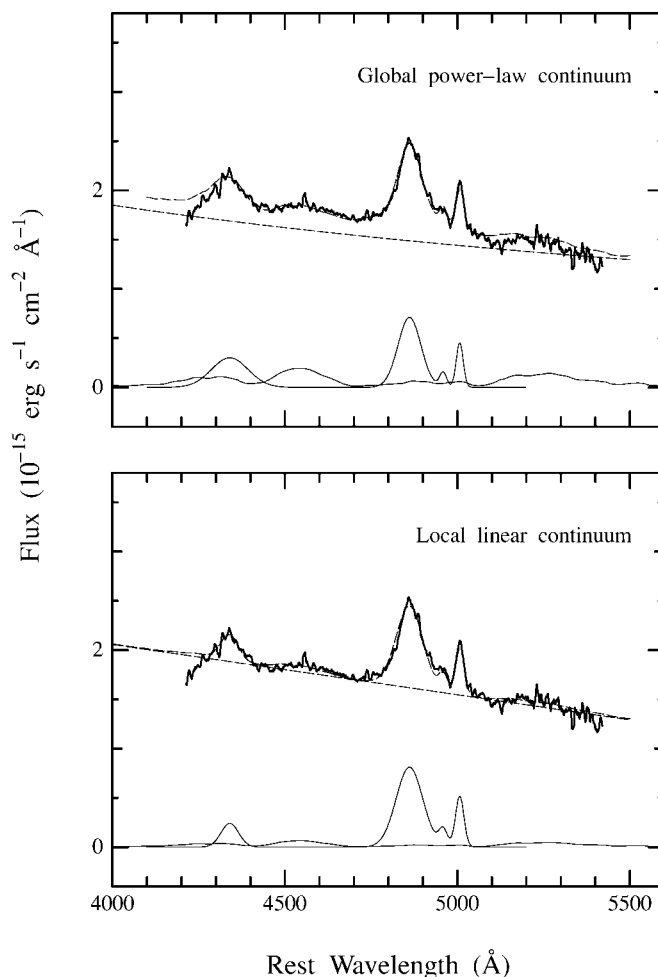


FIG. 4.—Profile fit of the K-band spectrum. *Top*, the result using the global power-law continuum; *bottom*, the result using the local continuum. Note that the flux is multiplied by $1 + z$ for deredshifting.

continuum fits. Therefore, we suggest that previous measurements of optical Fe II/H β ratios for low- z quasars and Seyfert nuclei may be underestimated by a factor of a few. We also note that a local continuum fit should be used if one would like to first compare new results with previous published values.

REFERENCES

- Boroson, T. A., & Green, R. F. 1992, *ApJS*, 80, 109
 Carswell, R. F., et al. 1991, *ApJ*, 381, L5
 Elias, J. H., Frogel, J. A., Matthews, K., & Neugebauer, G. 1982, *AJ*, 87, 1029
 Elston, R., Thompson, K. L., & Hill, G. J. 1994, *Nature*, 367, 250
 Francis, P. J., Hewett, P. C., Foltz, C. B., Chaffee, F. H., Weymann, R. J., & Morris, S. L. 1991, *ApJ*, 373, 465
 Hill, G. J., Thompson, K. L., & Elston, R. 1993, *ApJ*, 414, L1
 Hodapp, K.-W., et al. 1996, *NewA*, 1, 177
 Hora, J. L., & Hodapp, K.-W. 1996, *Observer's Guide for KSPEC* (Honolulu: Univ. Hawaii, Inst. Astron.)
 Hyland, A. R., Becklin, E. E., & Neugebauer, G. 1978, *ApJ*, 220, L73
 Impey, C. D., Foltz, C. B., Petry, C. E., Browne, I. W. A., & Patnaik, A. R. 1996, *ApJ*, 462, L53
 Jim, K. T. C., et al. 1999, in preparation
 Kawara, K., Murayama, T., Taniguchi, Y., & Arimoto, N. 1996, *ApJ*, 470, L85 (K96)
 Kundić, T., Hogg, D. W., Blandford, R. D., Cohen, J. G., Lubin, L. M., & Larkin, J. E. 1997, *AJ*, 114, 2276
 Lançon, A., & Rocca-Volmerange, B. 1992, *A&AS*, 96, 593
 Lawrence, C. R., Neugebauer, G., Weir, N., Matthews, K., & Patnaik, A. R. 1992, *MNRAS*, 259, 5P
 Lipari, S., Terlevich, R., & Macchetto, F. 1993, *ApJ*, 406, 451
 Murayama, T., Taniguchi, Y., Evans, A. S., Sanders, D. B., Ohya, Y., Kawara, K., & Arimoto, N. 1998, *AJ*, 115, 2237
 Patnaik, A. R., Browne, I. W. A., Walsh, D., Chaffee, F. H., & Foltz, C. B. 1992, *MNRAS*, 259, 1P
 Puetter, R. C., Smith, H. E., Willner, S. P., & Pipher, J. L. 1981, *ApJ*, 243, 345
 Soifer, B. T., Neugebauer G., Oke, J. B., & Matthews, K. 1981, *ApJ*, 243, 369
 Taniguchi, Y., Arimoto, N., Murayama, T., Evans, A. S., Sanders, D. B., & Kawara, K. 1997a, in *Quasar Hosts*, ed. D. L. Clements & I. Pérez-Fournon (Berlin: Springer), 122
 Taniguchi, Y., Murayama, T., Kawara, K., & Arimoto, N. 1997b, *PASJ*, 49, 419
 Turnshek, D. A., et al. 1994, *ApJ*, 428, 93
 Wills, B. J., Netzer, H., & Wills, D. 1985, *ApJ*, 288, 94
 Yee, H. K. C., & Bechtold, J. 1996, *AJ*, 111, 1007
 Yoshii, Y., Tsujimoto, T., & Nomoto, K. 1996, *ApJ*, 462, 266